

**Figure 1.** Structure and labeling scheme for  $\text{Me}_2\text{ClGe}(\text{S}_2\text{CNMe}_2)$  (50% probability for thermal ellipsoids). Hydrogen atoms are drawn arbitrarily small. Bond distances and angles are compiled in Table III.

195.6 relative to tetramethylsilane.<sup>9,10</sup> The vibrational spectra show the following features ( $\text{cm}^{-1}$ ):  $\nu(\text{CS})_2$  (asymmetric and symmetric) at 1168 and 1002;<sup>1,2,11</sup>  $\nu(\text{GeC}_2)$  (asymmetric and symmetric) at 635 (627 Raman) and 581 (574 Raman);<sup>8,12</sup>  $\nu(\text{GeS})$  at 418 (423 Raman).<sup>13</sup> Thus, a monodentate ligand is suggested with a pseudotetrahedral arrangement about germanium. The only peak attributable to  $\nu(\text{GeCl})$  is at 315  $\text{cm}^{-1}$  (310 Raman), which suggests a relatively weak Ge-Cl bond as found for the axial Ge-Cl bond in the trigonal-bipyramidal structure of  $\text{Cl}_4\text{Ge-NMe}_3$ .<sup>12,14,15</sup> These apparently conflicting pieces of information indicated the need for a structural determination (Figure 1).

The Ge atom in  $\text{Me}_2\text{ClGe}(\text{S}_2\text{CNMe}_2)$  is essentially at the center of a distorted trigonal bipyramid, with the two C atoms of the methyl groups and one of the S atoms occupying the equatorial positions. The Cl atom clearly occupies one axial position while the second S atom of the dithiocarbamate ligand occupies the second axial site but at a distance much greater than expected for a normal covalent Ge-S bond, forming an angle of 159.2 (1) $^\circ$  rather than 180 $^\circ$  with the Ge-Cl bond.

The Ge-C bond lengths (1.929 (2), 1.925 (2) Å) are typical of all methylgermanes and remarkably close to those found in  $\text{Me}_2\text{GeCl}_2$  (1.928 (6) Å).<sup>16</sup> Similarly, the peaks assigned to the  $\text{GeC}_2$  stretches are close to those assigned for  $\text{Me}_2\text{GeCl}_2$  (634, 592  $\text{cm}^{-1}$ ).<sup>12</sup> The Ge-S bond in the equatorial plane is of a length (2.254 (1) Å) expected from the sum of the covalent radii of Ge and S (2.25 Å),<sup>17</sup> and the value of  $\nu(\text{GeS})$  is close to that expected for a normal Ge-S bond.<sup>13</sup> By contrast, the Ge-Cl bond (2.251 (1) Å) is appreciably longer than it is in  $\text{Me}_2\text{GeCl}_2$  (2.143 (4) Å)<sup>16</sup> but remarkably close to the length of the axial Ge-Cl bond in  $\text{Cl}_4\text{Ge-NMe}_3$  (2.24 (1) Å).<sup>14</sup> The assignment of GeCl to 315  $\text{cm}^{-1}$  is therefore reasonable and consistent with the presence of a weaker Ge-Cl bond. Furthermore, the Ge-S distance (2.896 (1) Å) for the second S atom is so long that a second peak in the Ge-S stretching region cannot be expected.

The C-Ge-C angle is hardly changed (121 (4)-121.9 (1) $^\circ$ ) when one of the Cl atoms in  $\text{Me}_2\text{GeCl}_2$  is substituted by the

dithiocarbamate ligand. If the reaction originates by a nucleophilic attack by a S atom along the  $\text{C}_2$  axis bisecting the Cl-Ge-Cl angle in  $\text{Me}_2\text{GeCl}_2$ , then this equatorial S atom virtually remains at its attacking position, the  $\text{CH}_3$  groups are unaffected, the remaining Cl atom is bent back to the axial position of a trigonal bipyramid, and the vacant site on the opposite side is partly occupied by the second S atom. Presumably, with a monodentate attachment, the S and Cl atoms would simply rearrange to a pseudotetrahedral arrangement. However, the molecule is apparently "frozen" in this intermediate structure to give anisobidentate coordination. The structure is similar to that of  $\text{Me}_2\text{ClSn}(\text{S}_2\text{CNMe}_2)$ ,<sup>3</sup> although the C-Sn-C angle is considerably larger (128 (2) $^\circ$ ) and the axial Cl-Sn-S angle smaller (154.5 (4) $^\circ$ ) than the corresponding angles in the Ge analogue. Both distortions seem surprising because a closer adherence to 120 and 180 $^\circ$  angles might be anticipated on the larger Sn atom.

**Acknowledgment.** This research was sponsored in part by a Strategic Grant from the Natural Sciences and Engineering Research Council of Canada.

**Registry No.**  $\text{Me}_2\text{ClGe}(\text{S}_2\text{CNMe}_2)$ , 93304-69-9;  $\text{Me}_2\text{GeCl}_2$ , 1529-48-2;  $\text{Me}_2\text{NCS}_2\text{Na}$ , 128-04-1.

**Supplementary Material Available:** Tables of anisotropic thermal parameters, hydrogen atom coordinates and isotropic thermal parameters, and observed and calculated structure factors (10 pages). Ordering information is given on any current masthead page.

Contribution from the Department of Chemistry, Kansas State University, Manhattan, Kansas 66506

### Interligand Frontier Orbital Contacts in Phenanthroline Chelates

Keith F. Purcell

Received May 7, 1984

The idea of intermolecular contacts as a basis for phase transitions in solids is relatively unexplored. Recent interest in cooperative intersystem crossing in Fe(II) chelates containing phenanthroline as a ligand<sup>1</sup> and in solid-state racemization of phenanthroline-containing chelates<sup>2</sup> has prompted our study of a frontier orbital basis for interligand contacts in such materials. We report here a striking correspondence between the stereochemistry of the cation packing in  $\text{Fe}(\text{phen})_3\text{I}_2 \cdot 2\text{H}_2\text{O}$  and the  $\pi$  HOMO/LUMO topologies of the phenanthroline molecule.

Using literature values<sup>3</sup> of the bond distances and bond angles of the coordinated phenanthroline molecule, we have carried out a full valence electron INDO calculation to determine the ligand  $\pi$  HOMO and  $\pi$  LUMO topologies. Both perspective and contour plots of the wave probability functions ( $\psi^*\psi$ ) are shown in Figure 1.<sup>4</sup> These functions are readily identifiable as  $\pi$  and  $\pi^*$  types for the ethylene linkage that bridges the two pyridyl rings of phenanthroline (adjacent closed contour regions have opposite signs of  $\psi$ ). Clearly there is also well-developed delocalization of the HOMO and LUMO

(9) Drake, J. E.; Glavincevski, B. M.; Humphries, R. E.; Majid, A. *Can. J. Chem.* **1979**, *57*, 1426.

(10) Levy, G. C.; Lichter, R. L.; Nelson, G. L. "Carbon-13 Nuclear Magnetic Resonance Spectroscopy"; Wiley: New York, 1980.

(11) Sharma, C. P.; Kumar, N.; Khandpal, M. C.; Chandra, S.; Bhide, V. G. *J. Inorg. Nucl. Chem.* **1981**, *43*, 923.

(12) Griffiths, J. E. *Spectrochim. Acta* **1964**, *20*, 219.

(13) Drake, J. E.; Glavincevski, B. M.; Henderson, H. E.; Hemmings, R. T. *Can. J. Chem.* **1978**, *56*, 465.

(14) Bilton, M. S.; Webster, M. J. *Chem. Soc., Dalton Trans.* **1972**, 722.

(15) Beattie, I. R.; Ozin, G. A. *J. Chem. Soc. A* **1970**, 370.

(16) Drake, J. E.; Hencher, J. L.; Shen, Q. *Can. J. Chem.* **1977**, *55*, 1104.

(17) Cotton, F. A.; Wilkinson, G. "Advanced Inorganic Chemistry"; Wiley: New York, 1980.

(1) (a) Edwards, M. P.; Hoff, C. D.; Curnutte, B.; Eck, J. S.; Purcell, K. F. *Inorg. Chem.* **1984**, *23*, 2613. (b) Purcell, K. F.; Edwards, M. P. *Inorg. Chem.* **1984**, *23*, 2620. (c) Haddad, M. S.; Federer, W. D.; Lynch, M. W.; Hendrickson, D. N. *Inorg. Chem.* **1981**, *20*, 123, 131. Gutlich, P. *Struct. Bonding (Berlin)* **1981**, *44*, 83. König, E.; Ritter, G.; Kulshreshtha, S. K. *Inorg. Chem.* **1984**, *23*, 1144.

(2) Fujiwara, T.; Yamamoto, Y. *Inorg. Chem.* **1980**, *19*, 1903.

(3) Frenz, B. A.; Ibers, J. A. *Inorg. Chem.* **1972**, *11*, 1109.

(4) The plots were generated on the Kansas State University Computing Center's Calcomp plotter using the program SURFACE II by R. J. Sampson (available from the Kansas Geological Survey, The University of Kansas, Lawrence, KS 66044).

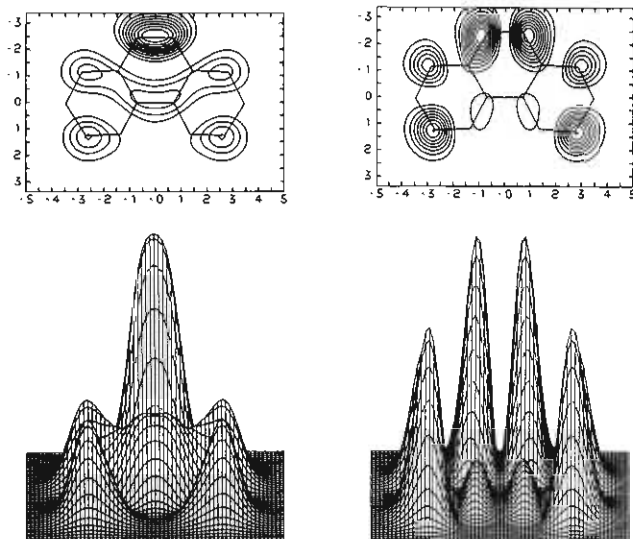


**Figure 1.** Contour maps and perspective views of the phenanthroline HOMO and LUMO point probability density functions in a plane parallel to that of phen and 150 pm above it. The maximum point electron probability ( $P$ ) has been scaled to 1.0 in both cases, and the contours are drawn at  $0.1P$  intervals. In both cases the INDO wave functions were renormalized to include overlap prior to the probability density calculations.

FE (PHEN) 312

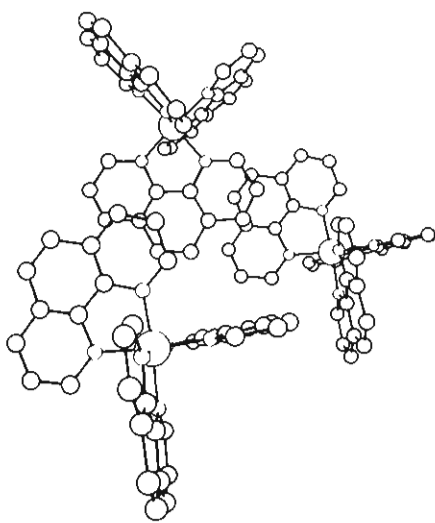


**Figure 2.** View, with perspective, normal to the parallel planes of phen ligands believed to be in contact in  $\text{Fe}(\text{phen})_3\text{I}_2 \cdot 2\text{H}_2\text{O}$ . Only a three-chelate segment of the chain is displayed.

waves into the pyridyl rings at the  $\alpha$  and  $\gamma$  positions, which turns out to be an important characteristic of the HOMO and LUMO in the context of chelate packing.

Next we turn to the molecular packing reported for  $\text{Fe}(\text{phen})_3\text{I}_2 \cdot 2\text{H}_2\text{O}$ .<sup>5</sup> The reported atom coordinates (in the  $P2_1/a$  unit cell axis system) have been transformed to a Cartesian system, and a perspective view of the cation packing is given in Figure 2; specifically, this view is normal to the planes of those phen ligands we felt might be involved in "charge-transfer" interactions. It is easily seen from this perspective that the chelate chain is comprised of a zigzag arrangement of cations, with the chain axis canted at an angle to the projection plane. The  $\text{I}^-$  anions appear to have no

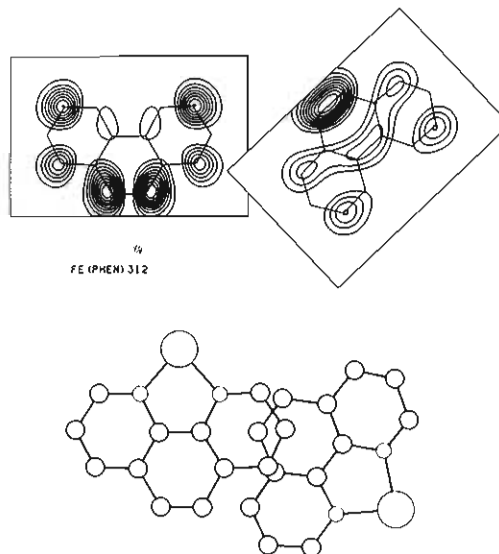


**Figure 3.** Bottom: Two-chelate segment of the chelate chain, without perspective, shown in Figure 2. Top: Exploded view of the phenanthroline HOMO and LUMO contours with the phen ligands oriented as in the bottom portion of this figure.

interactions with the cations; the  $\text{I}^-$  and  $\text{H}_2\text{O}$  moieties interact via hydrogen bonds to form chains paralleling and separating the cation chains. The closest  $\text{H}_2\text{O}$  molecule is situated along a pseudo- $C_3$  axis at an  $\text{Fe}-\text{O}$  distance of 488 pm.<sup>5</sup>

To examine more closely the phen/phen contacts, we carried out the projection without perspective and limited the projection to the unique phen ligand of the central chelate and that of the chelate immediately below it (Figure 3, bottom). The relation of this contact to that of the central phen and the phen immediately above it is simply that of an ethylene/ $\alpha,\gamma$  switch. The striking aspect of this projection is the involvement of the ethylene bridge functions and the  $\alpha$  and  $\gamma$  atoms within the pyridyl rings.

To complete the association of the chelate packing with the  $\pi$  HOMO/LUMO topologies, we show at the top of Figure 3 an exploded view of the central phen  $\pi$  LUMO and its nearest neighbor  $\pi$  HOMO, in the same relative orientations as given at the bottom of Figure 3. It is at once obvious that the  $\pi$  HOMO/ $\pi$  LUMO nodal surfaces are topologically well matched, with nearly coincident nodal surfaces in the contact region. Given that the inter-phen spacing is only 350 pm (cf. 362 pm in TTF and 347 pm in TTF·TCNQ<sup>6</sup>), it is an inescapable conclusion that a weak donor-acceptor interaction of the anticorrelated type<sup>7</sup> between chelates exists in  $\text{Fe}(\text{phen})_3\text{I}_2 \cdot 2\text{H}_2\text{O}$ .

We feel that a variety of solution and solid-state chemical and physical phenomena are traceable to, or at least influenced by, such frontier orbital interactions in phenanthroline-bearing chelates. The interleaving of  $[\text{Cu}(\text{dmphen})(\text{CN})]_n$  chains (dmphen = 2,9-dimethylphenanthroline) is characterized by 326-pm contacts of the dmphen ligands.<sup>8</sup> The interleaving of nitrobenzene molecules between phen ligands in  $\text{Fe}(\text{phen})_3\text{I}_2 \cdot 2\text{H}_2\text{O} \cdot \text{C}_6\text{H}_5\text{NO}_2$ <sup>9</sup> finds a natural explanation through such charge-transfer interactions, and Yamamoto believes<sup>10</sup> the association exists in solution, where it has a significant effect on the rate of chelate racemization. The molecular

(5) Johansson, L.; Molund, M.; Oskarsson, A. *Inorg. Chim. Acta* **1978**, *31*, 117.

(6) Wudl, F. *Acc. Chem. Res.* **1984**, *17*, 227. Kistenmacher, T. J. *Ann. N.Y. Acad. Sci.* **1978**, *312*, 333.

(7) Stevens, B. *Chem. Phys. Lett.* **1984**, *107*, 235.

(8) Morpurgo, G. O.; Dessy, G.; Fares, V. *J. Chem. Soc., Dalton Trans.* **1984**, 785.

(9) Fujiwara, T.; Iwamoto, E.; Yamamoto, Y. *Inorg. Chem.* **1984**, *23*, 115.

(10) Iwamoto, E.; Fujiwara, T.; Yamamoto, Y. *Inorg. Chim. Acta* **1980**, *43*, 95.

packing in materials such as  $\text{Fe}(\text{phen})_2(\text{NCS})_2$ , famous as the first example of a highly cooperative, thermally induced intersystem crossing chelate,<sup>11</sup> has not been reported. Were the packing to be analogous to that of the parent  $\text{Fe}(\text{phen})_3^{2+}$  cations discussed here, a simple chemical basis for the cooperativity would exist: the electron density rearrangement within a chelate that experiences the singlet-quintet intersystem crossing would be communicated to both nearest-neighbor chelates. More quantitatively, the finding that  $\Delta H$  is positive and is on the order of 4 kJ/mol<sup>1b</sup> for the local reaction singlet $\cdots$ singlet  $\rightarrow$  singlet $\cdots$ quintet finds a logical explanation in the frontier orbital interaction described here.

It is important to note further that the phen  $\pi$  HOMO and  $\pi$  LUMO are mixed with the metal  $d\pi$  AOS, themselves directly involved in the orbital occupation change ( $d\pi^6d\sigma^0 \rightarrow d\pi^4d\sigma^2$ ) accompanying the singlet-quintet conversion. Other ramifications, such as the possibilities for thermal, chemical, and photoinduced conductivities in solids analogous to those discussed here, are under consideration in our laboratory.

**Acknowledgment** is made to the donors of the Petroleum Research Fund, administered by the American Chemical Society, for support of this work.

**Registry No.**  $\text{Fe}(\text{phen})_3\text{I}_2 \cdot 2\text{H}_2\text{O}$ , 42992-96-1.

(11) König, E.; Madeja, K. *Inorg. Chem.* **1967**, *6*, 48. Sorai, M.; Seki, S. *J. Phys. Chem. Solids* **1974**, *35*, 555.

Contribution from the Anorganisch-Chemisches Institut, Universität Zürich, CH-8057 Zürich, Switzerland

### Comment on the Measurement and Interpretation of Susceptibility Data

Philippe Baltzer\* and Jürg Hulliger

Received June 5, 1984

The aim of this paper is to draw the chemists attention to some aspects of experimental magnetochemistry. For magnetic investigations, Faraday balances, SQUID magnetometers, etc., equipped with superconducting solenoids and low-temperature accessories are quite common nowadays. Since they are working at high magnetic fields and temperatures even below 4 K, substantial complications in the measurement and interpretation are expected for many magnetic compounds. We therefore discuss two important aspects: (i) "orientation effect" in magnetically anisotropic, loosely packed powder samples (see also ref 2 and 3); (ii) nonlinear field effects at low temperatures and in high fields.<sup>1</sup>

(i) Any magnetically anisotropic particle is subject to a torque if placed in a homogeneous magnetic field. This torque tends to align crystallites with the magnetic axis of maximum magnetization parallel to the field (see i.e., ref 3). The effect is opposed by mechanical friction forces between the particles of the sample and hence can be avoided by increasing this force. Since the torque is proportional to the anisotropy of magnetization and to the square of the field strength, pronounced effects are expected at low temperature and in high

- (1) (a) Vermaas, A.; Groeneveld, W. L. *Chem. Phys. Lett.* **1974**, *27*, 583. (b) Marathe, V. R.; Mitra, S. *Chem. Phys. Lett.* **1974**, *27*, 103.
- (2) Mulay, L. N. In "Physical Methods of Chemistry"; Wiley-Interscience: New York, 1972; Part IV, p. 431 ff.
- (3) Hulliger, J.; Zoller, L.; Ammeter, J. H. *J. Magn. Reson.* **1982**, *48*, 512.

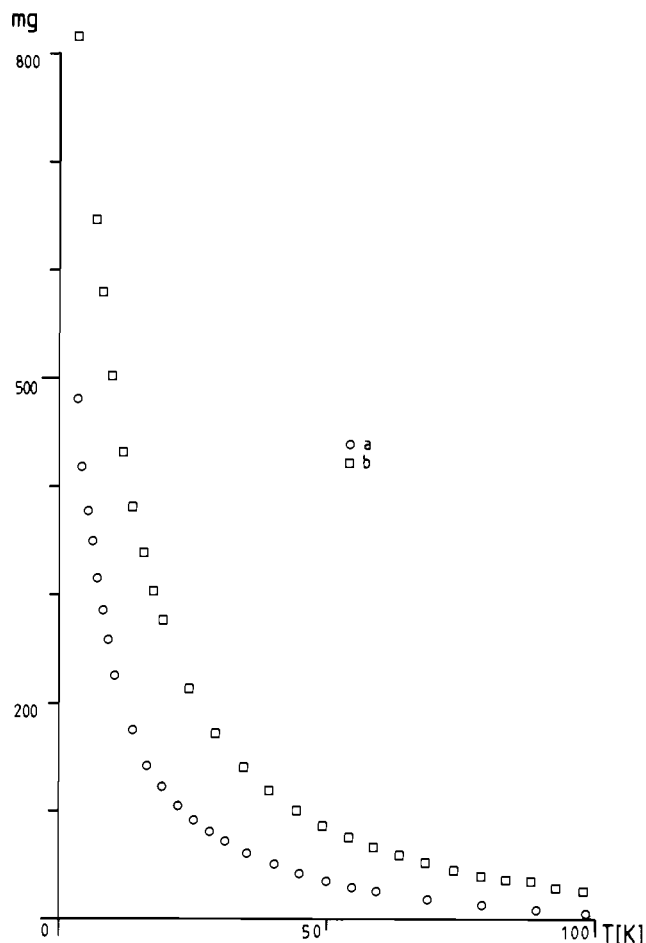


**Figure 1.** Measured effect on the microbalance of a Faraday setup calibrated to 1 g of a powder sample of 5% decamethylmanganocene in decamethylruthenocene at 6.19 T and  $0.7 \text{ T cm}^{-1}$ : (a) mechanically fixed; (b) oriented in high magnetic field (see text).

fields. Figure 1 shows that even in the case of a magnetically diluted sample, a partial orientation of crystallites can take place. Curve a represents the data from a mechanically fixed powder, whereas curve b was obtained from a loosely packed sample, slightly shaken at 4 K and 6.2 T before measurement.

The same behavior has been observed for the well-known calibration standard  $\text{HgCo}(\text{NCS})_4$  (MTC). The measured effect on a Faraday balance for this compound increased about 10% even at 200 K when a loosely packed powder was treated as described above. This might explain the quite different low-temperature results reported for MTC.<sup>4</sup> A magnetically anisotropic compound should therefore be mechanically fixed, when used as a calibrant in modern susceptibility setups. Throughout our investigations we performed this mechanical fixation with the simple tool shown in Figure 2.

A cylindrical sample holder made from aluminum foil<sup>5</sup> (common household foil), put into the cavity (O), is filled with the powdered material. The screw (M8) and the plug (ST) press the sample to the bottom. This augments the mechanical friction forces within the sample. The pressed sample and the sample holder can then be removed by means of screw (M3). Finally, the sampleholder is shut by pressing together the open top of the aluminum cylinder.

On the other hand, the orientation effect may also favor an investigation if an almost perfect alignment can be achieved.

- (4) Bünzli, J. C. *Inorg. Chim. Acta Lett.* **1979**, *36*, 413.
- (5) Compared with a usual sample holder made of quartz glass with similar dimensions, our sample holder is much lighter (about 10 times) and therefore its effect on the measured susceptibility is much smaller.